Impact of Lake/reservoir Expansion and Shrinkage on Energy and Water Vapor Fluxes in the Surrounding Area

Ailun Guo[1,2], Shaomin Liu[1*], Zhongli Zhu[1], Ziwei Xu[1], Qing Xiao[3], Qian Ju[1], Yuan Zhang[1], Xiaofan Yang[1]

1. State Key Laboratory of Earth Surface Processes and Resource Ecology, Faculty of Geographical Science, Beijing Normal University, Beijing 100875, China.

2. College of Urban and Environmental Sciences, Peking University, Beijing 100871, China.

3. State Key Laboratory of Remote Sensing Science, Aerospace information research institute, Chinese Academy of Sciences, Beijing 100101, China

Submitted to "**Journal of Geophysical Research: Atmospheres**"

Corresponding to: Dr. Shaomin Liu, E-mail: smliu@bnu.edu.cn

Key Points:

- The Guanting Reservoir expanded annually from 2013 to 2017, and it expanded in spring, shrank in summer, and expanded again in winter.
- The expansion and shrinkage of the reservoir affect evapotranspiration through the ratio of water bodies, net radiation and soil moisture.
- The difference in ET between the closer site and further site increased with reservoir expansion, especially in the non-growing season.

Abstract:

Lakes and reservoirs are important components of freshwater. The expansion and shrinkage of lakes/reservoirs may alter meteorological characteristics and the underlying surface conditions, which would further affect energy and water vapor fluxes in the surrounding area. In this study, the expansion and shrinkage of the Guanting Reservoir during 2013-2017 was analyzed using remote sensing data. Data collected from the Huailai Remote Sensing Experiment Station were used to analyze the energy and water vapor fluxes. The results showed the annual expansion of the Guanting Reservoir from 2013 to 2017, and a seasonal variation characterized by expansion in spring, shrinkage in summer and autumn, and expansion again in winter was exhibited. Meanwhile, the evapotranspiration (ET) in the surrounding area also increased annually. In the growing season, the seasonal shrinkage of the reservoir indirectly affected ET through net radiation, deep soil moisture and vegetation growth conditions, while in the non-growing season, the seasonal expansion directly increased ET by increasing the proportion of water bodies in the source area and increased net radiation and surface soil moisture. In addition, with the reservoir expanding year by year, the difference in ET between the closer site and further site from the reservoir increased obviously, especially in the non-growing season during the seasonal expansion of the reservoir. The results help with the ecosystem restoration and sustainable development of lakes/reservoirs in arid and semiarid areas.

1. Introduction

Lakes and reservoirs only occupy approximately 4% of the global terrestrial surface (Downing et al. 2006), but they are of great importance due to their significant contributions to the water supply (Lee et al. 2014). In arid and semiarid regions of China, lakes and reservoirs provide major freshwater resources for inland watersheds and basins. Previous studies have indicated that the expansion and shrinkage of lakes/reservoirs are not only caused by climate change (Williamson et al., 2009; Xiao et al., 2018) but also by human activities (e.g., agricultural irrigation, dam construction and water conservancy projects) (Guo et al., 2008, 2012; Shi et al. 2012; Ruan et al., 2012; Haddeland et al. 2014; Shadkam et al., 2016; Xie et al., 2017). In turn, the expansion and shrinkage of lakes/reservoirs would also have an impact on the local microclimate and thus affect crop yields and agricultural development in the surrounding areas (Min et al., 1995).

The lake effect is a function of the climatic conditions in which a lake is situated, the local setting of the lake and its surroundings and the morphometry of the lake itself (Kodama et al., 1983). Since lakes/reservoirs act differently than surrounding lands in the exchanges of radiation and energy and water vapor, these water bodies influence local, regional and even global climates (Bates et al., 1993; Rouse et al., 2005; Liu et al., 2012; Biermann et al., 2014; Li et al., 2016). For example, the lake effect of Lake Minchumina led to a longer growing season than other stations in interior Alaska, which showed the lake's warming effect in the surrounding areas (Kodama et al., 1983). Additionally, the large thermal contrast between lakes/reservoirs and their surrounding lands often triggers thermal circulation, which has a significant impact on energy and water vapor transport (Lee, et al., 2014).

Currently, hydrometeorological observations are obtained to measure surface energy and water vapor fluxes, and these measurement devices include lysimeters, the Bowen ratio energy balance system, the eddy covariance system (EC), scintillometers, and so on (Liu et al., 2013). However, long-term (>1 yr) measurements of surface energy and water vapor fluxes for lake/reservoir systems have remained challenging until recently (Liu et al., 2012; Lee et al. 2014). In recent years, through direct observations of energy and water vapor fluxes on lakes/reservoirs, previous studies have analyzed the characteristics of water-atmosphere interactions on lakes/reservoirs, including the surface energy budget (Li et al., 2016), carbon cycle (Vesala et al., 2006), and energy balance closure (Nordbo et al., 2011; Wang et al., 2017). Furthermore, the energy and water vapor fluxes of two kinds of underlying surfaces, water and land surfaces, have been compared, including lake/desert, lake/forest, and lake/farmland surfaces (Liu et al., 2008). For example, using the EC technique, the latent and sensible heat fluxes from lake and forest surfaces were compared in two lakes in central Sweden (Venäläinen et al., 1998), as well as in Lake Valkea-Kotinen in southern Finland (Vasala et al., 2006; Nordbo et al., 2011). The differences between the meteorological characteristics (such as energy distribution and turbulence intensity) of lake and desert surfaces were also analyzed in the Badan Jaran Desert (Ma et al., 2012; Ao et al., 2013; Zhang et al., 2014). However, these studies analyzed the energy and water vapor fluxes over either water or land surfaces, rather missing the interactions between the lake/reservoir and land surfaces.

In arid and semiarid areas with less precipitation and little vegetation in China, human activities play a dominant role in the expansion and shrinkage of lakes/reservoirs. Guanting Reservoir is located in Huailai County, Hebei Province, China, adjacent to Beijing, which belongs to the semiarid area in the North China Plain (NCP). After its construction in 1954, the

Guanting Reservoir was seriously contaminated by industrial waste, and the water volume of the reservoir continued to decline until 2013 (Yang et al., 2016) (Figure 1), which was mainly caused by the increasing agricultural water consumption and hydraulic projects occurring in the upstream areas (Chen, 2007). In recent years, in preparation for the 24th Winter Olympic Games in Beijing, the government enforced environmental protection strategies and policies, which were expected to improve the water quality and water level of the Guanting Reservoir. This study aimed to analyze the responses of energy and water vapor fluxes to the expansion and shrinkage of lakes/reservoirs. First, remote sensing data were used to analyze the interannual and seasonal expansion and shrinkage of the Guanting Reservoir. Second, long-term large-aperture scintillometer (LAS) and automatic weather station (AWS) data were used to analyze the relationship between the expansion and shrinkage of the reservoir and the variations in energy and water vapor fluxes in surrounding areas. Finally, using EC and AWS data from two nearby observational sites, the variations in energy and water vapor fluxes at different distances from the reservoir were analyzed, and the influencing mechanism was discussed. This study also provides scientific implications for the ecosystem restoration and sustainable development of lakes/reservoirs in arid and semiarid areas.

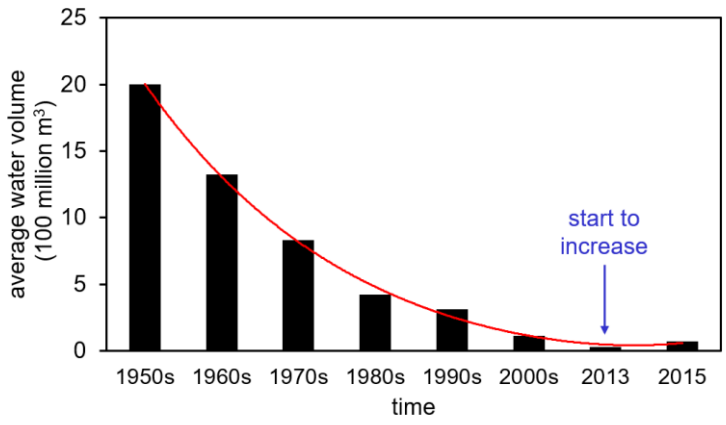

Figure 1. Variations in the water volume in the Guanting Reservoir from the 1950s to 2015 (the water volume data were adopted from Yang et al., 2015 and Chen et al., 2007).

2. Materials and Methods

2.1 Site Description and Measurements

The study area is on the southeastern shore of the Guanting Reservoir, which is in the middle reaches of the Hai River Basin. The study site was located in the Huailai Remote Sensing Experiment Station (latitude 40° 20' N, longitude 115° 47' E, Figure 2a), Hebei Province, China. The station is in the southwest area of the Yanqing-Huailai Basin, and on its north and south sides are northwest- to southeast-trending mountains. The climate is described as a temperate continental monsoon climate. The mean temperature is approximately 10.1 ℃, the maximum temperature in summer is approximately 39 ℃, and the minimum temperature in winter is below -20 ℃. The mean annual precipitation is approximately 370 mm, which is mainly concentrated in summer. The annual average wind speed is 3.4 m·s-1. The prevailing wind direction is west in winter and early spring, and it is southeast in summer and autumn (Yang et al., 2015). The soils in the study area are sandy alluvial soil, and the main crops are single-season maize, which is planted in early May and matures in mid-to-late September each year (Yang et al., 2015).

The experimental area has a range of approximately 2 km×1 km, which can be divided into irrigated and non-irrigated farmland and is shown bounded by the red lines in Figure 2b. The 10 m tower was on irrigated farmland, and the 40 m tower was on non-irrigated farmland. The observation variables used in this study and their configuration information are shown in Table 1. Specifically, a group of LASs, two sets with the transmitter and receiver exchanged for each other was installed in the northeast-southwest direction, and the field of view of the instruments, which can be defined by the source area (Liu et al., 2013), includes both irrigated and non-

irrigated fields. Two ECs and two AWSs were installed on both the 10 m and 40 m towers to observe sensible heat flux (H), latent heat flux (LE), and meteorological elements (including four-component radiation, precipitation, wind speed/direction, air temperature/humidity, soil temperature/moisture profile, and so on). In addition, seven layers of meteorological gradient observation systems were installed at the 40 m tower.

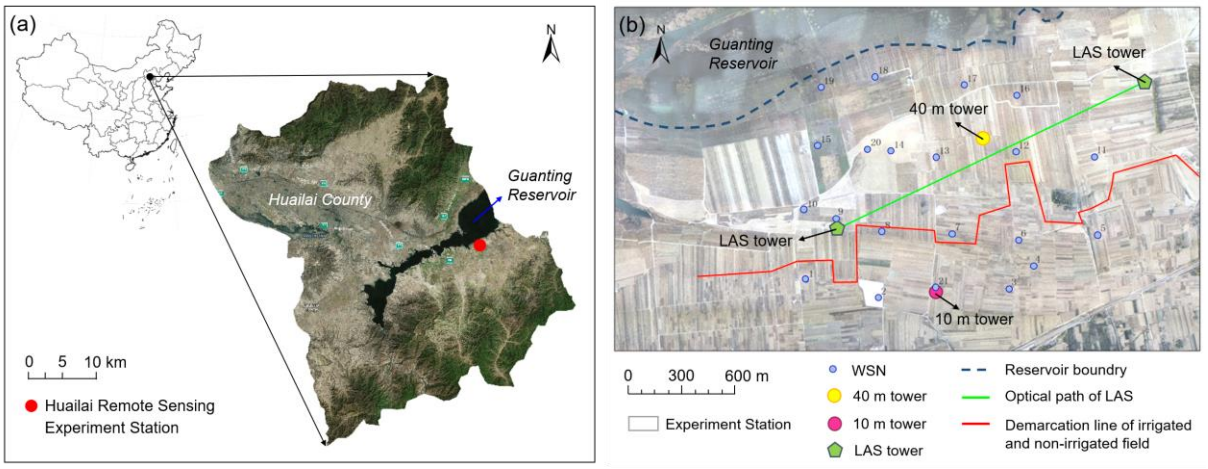

Figure 2. The Huailai Remote Sensing Experiment Station: (a) The location of the Huailai Remote Sensing Experiment Station, and (b) the observation system of the Huailai Experiment Station that was used in this study (the background image is the image of the surrounding area of the reservoir in 2013). The south side of the red line is the irrigated field, and the north side is the non-irrigated field.

Table 1. The observation instrument of the Huailai Experiment Station used in this study

Instrument	Variable	Site	Sensor Type	Height/Depth (m)
LAS	Sensible heat flux ($W\ m^{-2}$)	14m transmitting and receiving LAS tower	BLS450, Scintec, Germany; RR-RSS460, China	14 (path length: 1870m)
EC	Sensible heat flux and latent heat flux	on 10m tower	CSAT3&Li7500A, Campbell/Li-cor, USA	5

	($W\ m^{-2}$)	on 40m tower	CSAT3&EC150, Campbell, USA	3.5
AWS	Air temperature/humidity (℃, %)	on 10m tower	HMP45C, Vaisala, Finland	5
		on 40m tower	HMP155A, Vaisala, Finland	3,5,10,15,20,30,40
	Wind speed/direction ($m\ s^{-1}$, °)	on 10m tower	Ws03001, RM Young, USA	10
		on 40m tower	010C/020C, Met One, USA	3,5,10,15,20,30,40
	Soil heat flux ($W\ m^{-2}$)	1.5m from 10m tower	HFT3, Campbell, USA	0. 06
		3m from 40m tower	HFP01, Hukseflux, Netherland	0. 06
	Soil temperature/moisture profile (℃, %)	1.5m from 10m tower	AV-10TH, Avalon, USA	0.02,0.04,0.10,0.20, 0.40,0.80,1.20,1.60
			ECH_2O-5, Decagon Devices, USA	
		3m from 40m tower	109 CS616, Campbell, USA	0.02,0.04,0.10,0.20, 0.40,0.80,1.20,1.60
	Air pressure (hpa)	on 10m/40m tower	PTB110, Vaisala, Finland	5/10
	Precipitation (mm)	on 10m tower	TE525MM, Campbell, USA	10

	on 40m tower	TE525MM, Campbell, USA	2.8
Four-component radiation ($W\ m^{-2}$)	on 10m tower	CNR4, Kipp&Zonen, Netherland	5
	on 40m tower	CNR4, Kipp&Zonen, Netherland	4

2.2 Data Processing

Careful data processing and quality assessment are important to ensure the accuracy of the observation data and are critical for obtaining reliable results.

2.2.1 Flux and Meteorological Data

The LAS is a device that derives the turbulence intensity by measuring the refractive index of air (C_n^2) (Wang et al., 1978). Data were carefully screened to ensure the data quality of LAS observations, including [1] the exclusion of unreasonable data from raw C_n^2 data, [2] rejection of C_n^2 beyond the saturation criterion, [3] rejection of data with weak demodulated signals, and [4] rejection of data during periods of precipitation. Then, the sensible heat flux was iteratively calculated by combining meteorological data based on the Monin-Obukhov similarity theory (Liu et al., 2013). After the sensible heat flux was obtained, the latent heat flux/ET could be estimated from the energy balance equation, where the radiation and soil heat fluxes are the mean results at the two observation sites. There are two LAS set observations (BLS450 and RR-RSS460 obtained by Germany and China, respectively), and the data were primarily obtained from the BLS450 measurements; missing flux measurements from BLS450 were filled with measurements from RR-RSS460. A nonlinear regression method was used to fill the gaps to obtain the continuous ET.

The software Eddypro (LI-COR Company, https://www.licor.com/env/products/eddy_covariance/software.html) is used to process the EC data from 10 Hz, including spike removal, lag correction, performance of the planar fit coordinate rotation, frequency response correction, and so on. The EC data were averaged over 30-min periods and then screened (Li et al., 2018). In addition, the 30-min data were also filtered in a four-step procedure: [1] data from periods of sensor malfunction were rejected, [2] incomplete 30-min data were rejected when the missing data constituted more than 10% of the raw data record, [3] data within 1 h before or after precipitation were rejected, and [4] data at night when the turbulence was weak (u* less than 0.1 m/s) were rejected (Liu et al., 2011; Xu et al., 2013). To acquire the accumulative ET, the look-up table (LUT) method was used to fill the gaps, and the Bowen ratio closure method was used to force the energy balance (Liu et al., 2016).

The AWS data used in this study are listed in Table 1. In the data processing, data that are obviously beyond the range of physical possibilities are rejected, and the gaps are filled by the linear interpolation method (Jia et al., 2012). The soil heat flux plates at the 10 m and 40 m towers were buried at depths of 0.06 m, where one was buried in a maize field (G1), and the other two were buried in the soil surface (G2 and G3). The surface soil heat flux (G0) was calculated using the “PlateCal” approach (Liebethal et al., 2005) based on the combination of weighted vegetation fraction, soil temperature and moisture measured above the heat plates.

2.2.2 Remote Sensing Data

Landsat OLI (Operational Land Imager) data retrieved from the United States Geological Survey (USGS) website (https://earthexplorer.usgs.gov/) were used in this study, and the resolution was 30 m. We obtained 36 images in total, covering the Guanting Reservoir and its

surrounding area in 2013-2017. The data were corrected using ENVI 5.3 software, including cutting, radiometric calibration and FLAASH atmospheric correction. The normalized difference vegetation index (NDVI, with a resolution of 30 m) was calculated using the reflectance in the near-infrared (ρ_{NIR}) and red bands (ρ_R).

2.2.2 Footprint Model

The footprint is a function that describes the relationship between the spatial distribution of sources or sinks near the surface layer and the surface flux data measured by instruments, and the footprint can be estimated by the footprint model. The source area refers to the upwind area that has a major contribution to the flux observations and is the integral of the footprint function in a particular region. To estimate the flux footprint of EC, the method proposed by Kormann and Meixner (2001) was used, which is an Eulerian analytic flux footprint model (Liu et al., 2013). For LAS, the footprint can be described by a spatial weight function along its optical length, combining the footprint model for point fluxes with the path-weighting function of the LAS (Liu et al., 2011). In this study, we used daytime (6:00-22:00) footprints of EC and LAS during 2013-2017. The resolution of the source area was 30 m for both the EC and LAS measurements, and the flux contribution of the source area was set to 90%.

3. Results and Discussion

3.1 Expansion and Shrinkage of the Guanting Reservoir

The water areas on selected dates during the middle of the growing season (July to August) in 2013-2017 were used to analyze the interannual variations in expansion and shrinkage of the Guanting Reservoir, including 6 July 2013, 25 July 2014, 12 July 2015, 7 July 2016, and 17 July 2017. Using the supervised classification method, the water areas in the last five years were

198 extracted, and the distances between the reservoir and observation point (40 m tower) were
199 calculated.

200 Figure 3 shows the water area of the Guanting Reservoir, which shows that the reservoir
201 expanded after 2013. The water bodies of the reservoir in 2013 and 2017 were compared in
202 Figure 3f, which shows the overall variation. The northeastern part of the Guanting Reservoir
203 had the most significant expansion over five years, and the Huailai Experimental Station is
204 located in this area. This expansion in this area is because the topography of the northeast part of
205 the reservoir is wide and flat, while the southwest part is narrow and deep. Under the same
206 conditions of water volume change, the northeast part has the most significant expansion and
207 shrinkage.

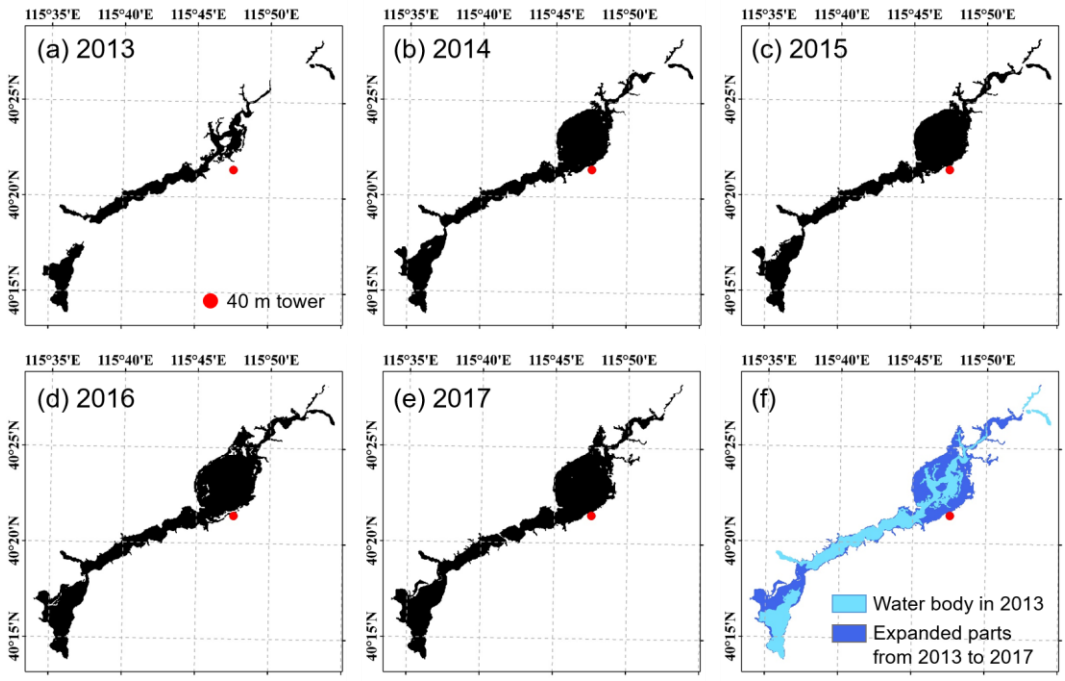

208

209 Figure 3. The ranges of the Guanting Reservoir: (a) - (e) the water body ranges from 2013 to 2017, and (f)
210 the comparison of the water body extents in 2013 and 2017.

Figure 4a shows the variations in water area and the distances between the reservoir and observation points in 2013-2017. From 47.21 km^2 in 2013 to 77.25 km^2 in 2017, the water area of the Guanting Reservoir increased gradually and had a total increase of 63.63%. In addition, with the increase in reservoir area, the distance between the 40 m tower and the reservoir gradually decreased from 720.7 m in 2013 to 289.4 m in 2017, which decreased by approximately 430 m in five years.

The interannual expansion and shrinkage of the Guanting Reservoir was closely related to the large hydraulic projects built in the upstream and the large agricultural water with low water use efficiency (Yang et al., 2015). According to Ma et al. (2014), during 1978-2013, the water area change in the Guanting Reservoir was weakly correlated with natural factors, such as precipitation and air temperature but was significantly negatively correlated with regional gross national product (GNP), especially the gross domestic product (GDP) of secondary industry and was significantly positively correlated with cultivated area. Therefore, the expansion and shrinkage of the Guanting Reservoir was mainly influenced by human factors, especially the interception/discharge of the reservoirs and the irrigation water use in the upstream area. For example, in Figure 4a, 2013-2014 is the fastest stage of the expansion. In these two years, the area of cultivated land in the upstream did not change significantly, but in October 2013 in the historical data, the Youyi Reservoir in the upstream started to transfer water to the Guanting Reservoir to meet the water supply demand in Beijing. The total water discharge reached 15 million m^3 (He et al., 2013), which directly led to the obvious expansion of the Guanting Reservoir in 2013-2014.

Since the distribution of precipitation is uneven during a year and the upstream water use changes seasonally, the area of the Guanting Reservoir also has seasonal variations. In this study,

234 we take 2015 as an example to analyze the seasonal variation in the expansion and shrinkage of
235 the Guanting Reservoir. Seven images from March to October were used to extract the water
236 body, including 22 March, 7 April, 25 May, 12 July, 13 August, 14 September and 16 October,
237 and the distances between the 40 m tower and reservoir were calculated. The results are shown in
238 Figure 4b. There was a rapid expansion from March to April, and then, the reservoir shrank from
239 June to July and expanded again in October. In 2015, the maximum water area of the Guanting
240 Reservoir appeared from April to May, with an area of approximately 68 km^2; the minimum area
241 of the reservoir occurred in September, which was approximately 64.4 km^2, and the reservoir
242 area changed by 3 km^2 during the year. The distance between the observation point and the
243 reservoir decreased sharply during the spring; in 2015, the distance decreased from 370 m to 336
244 m. From May to July, the distance increased gradually and reached its maximum, and in
245 October, the distance decreased again and reached its minimum, which was approximately 325
246 m in 2015. The distance between the observation point and the reservoir can be changed by
247 approximately 45 m within a year.

248 In a year, the variations in irrigation water upstream of the Guanting Reservoir are closely
249 related to the seasonal variation in the water area. The irrigation water was higher in the growing
250 season (summer and autumn) and lower in the non-growing season (winter and spring).
251 Therefore, the increase in irrigation water upstream made the Guanting Reservoir shrink, while
252 in the non-growing season, the decrease in irrigation water made the reservoir expand. In
253 addition, the precipitation in the growing season was larger than that of the non-growing season,
254 which led to a small increase in the reservoir area from August to September, as well as a small
255 decrease in the distance between the observation point and reservoir (Figure 4b).

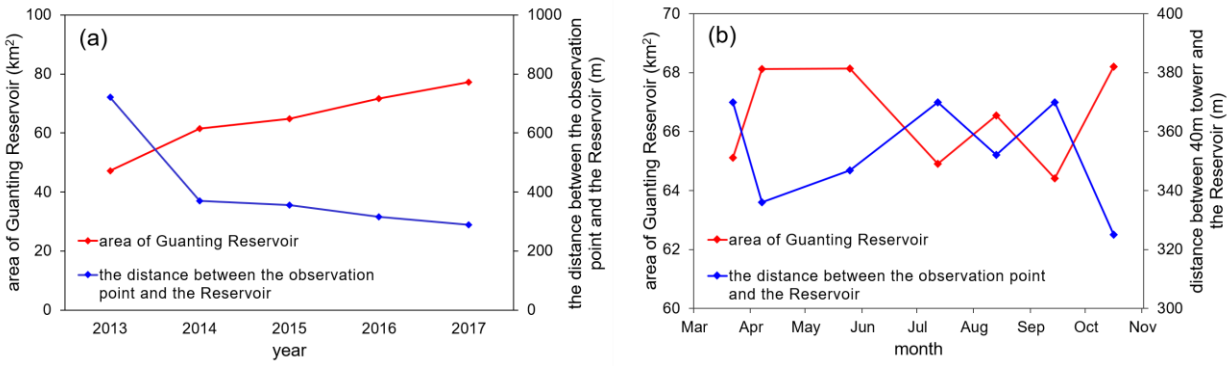

Figure 4. The interannual and seasonal variations in the Guanting Reservoir area and the distance between the observation point (40 m tower) and the reservoir from 2013 to 2017: (a) interannual and (b) seasonal.

3.2 Variations in Energy and Water Vapor Fluxes in the Surrounding Area of the Reservoir

The spatial scale of LAS measurement is kilometers, so this measurement can represent the average conditions at the regional scale. The LAS of the Huailai Experiment Station is 14 m high, and its path length is 1870 m. The 90% contribution source area of LAS has an average length of approximately 2000 m and a width of approximately 850 m, and the average area is approximately 1.7 km^2. Therefore, the characteristics of the LAS observations were used to represent the overall situation of water vapor and energy flux in the surrounding area of the Guanting Reservoir. In addition, the 40 m tower was located in the center of the LAS source area, so the meteorological elements observed by the 40 m tower can represent the meteorological characteristics of the area surrounding the reservoir.

3.2.1 The Variation in ET

The annual cumulative ET of the surrounding area from 2013 to 2017 was obtained by the daily ET data observed by LAS, and its variation is shown in Figure 5. From 2013-2017, the annual average ET in the surrounding area was approximately 656.3 mm and increased year by

year along with the expansion of the Guanting Reservoir, from 446.6 mm in 2013 to 874.7 mm in 2017. In the area surrounding the Guanting Reservoir, ET was mainly affected by meteorological factors and underlying surface conditions, including the area ratio of water bodies in the LAS source area, vegetation factors and soil factors. The expansion and shrinkage of the reservoir would also affect ET by affecting the meteorological characteristics.

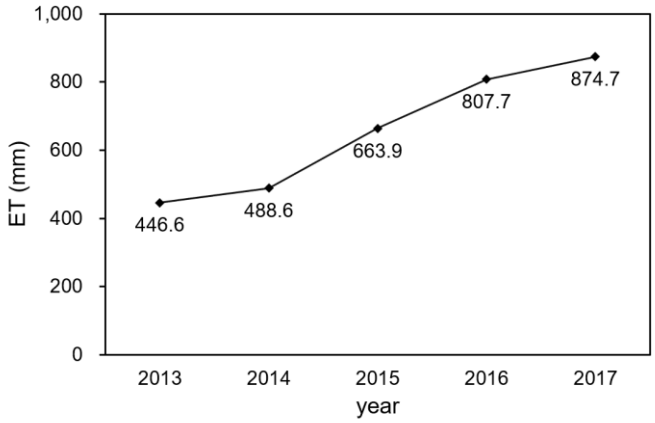

Figure 5. The interannual variation in annual ET observed by LAS from 2013 to 2017.

Figure 6 shows the change in the 90% contribution source area of LAS during the growing season from 2013 to 2017. Along with the expansion of the reservoir, the distance between the source area and the reservoir decreased significantly. From 2013-2015, there was no water body in the LAS source area. Until 2016 and 2017, the reservoir expanded to the interior of the LAS source area, and the area ratio of the water body was approximately 3.18% in 2016 and 1.33% in 2017 (Figure 6). The continuous expansion of the Guanting Reservoir changed the underlying surface of the LAS source area from a single farmland to a transition zone between water and farmland, increasing the proportion of water evaporation in the evapotranspiration (ET) of the source area. Therefore, the increase in the proportion of water bodies was the factor directly impacting on the increase in annual cumulative ET.

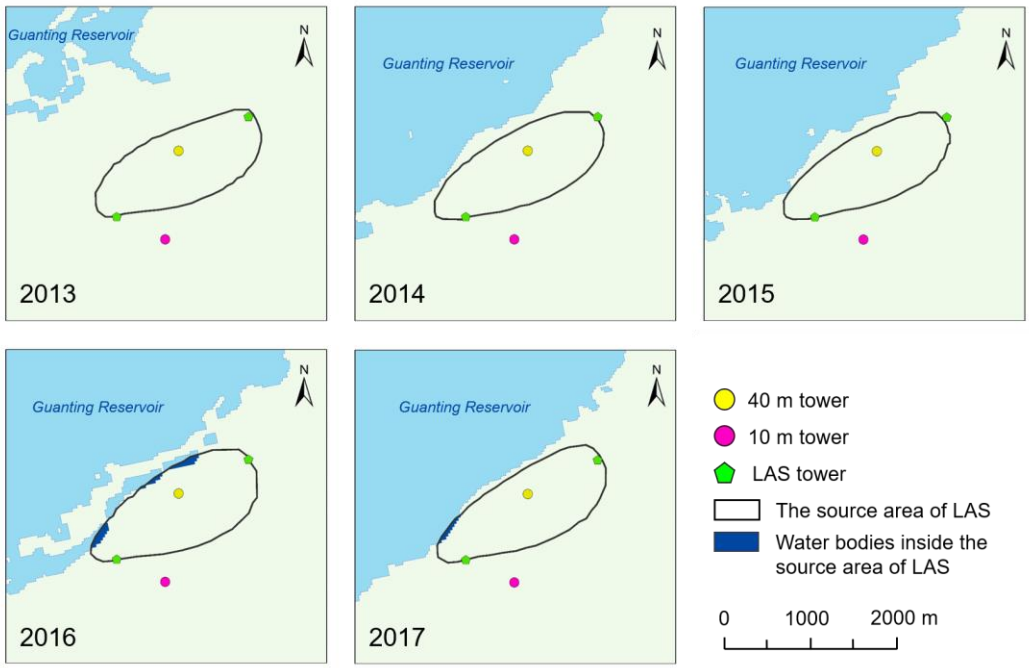

Figure 6. The interannual variation in annual ET observed by LAS from 2013 to 2017.

Figure 7 shows the seasonal variation in ET from 2013-2017. In one year, the ET first increased, reaching the maximum for the whole year in July-August, and then decreased to the minimum in winter. Comparing the seasonal variations in ET in each year, we can divide this changing regularity into three stages: [1] in spring (January to June), the ET of the surrounding area in 2014-2017 was significantly larger than that in 2013 and increased year by year. [2] In summer and autumn (July to September), there was no significant increase in ET, except in 2014. [3] In winter (October to December), the ET again shows an increasing trend year by year, but not as obvious as the first stage; however, the ET in 2014 was lower than that in 2013. In addition, in 2013, ET reached its peak in August, but since the expansion of the Guanting Reservoir in 2014, the peak appeared early in July, and the peak value of the monthly ET also increased from 119.5 mm in 2013 to 138.7 mm in 2017. These changes in the seasonal variation in ET were consistent with the seasonal changes in the reservoir (which are shown in Figure 4b).

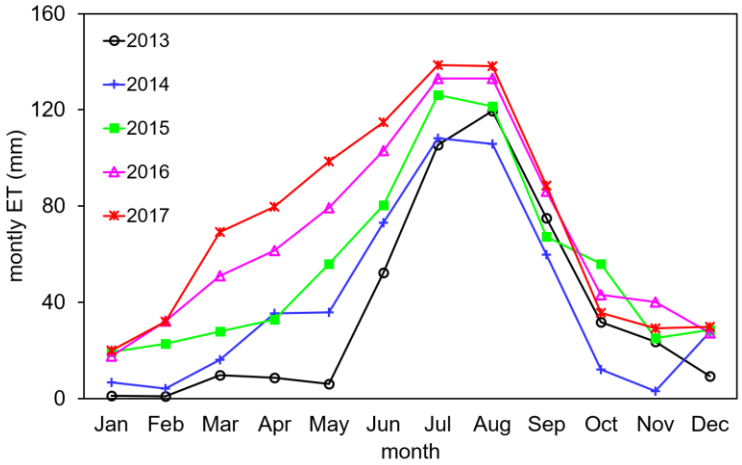

Figure 7. Seasonal variation in ET from 2013-2017.

Figure 8 shows the 90% contribution source area of LAS during spring, summer/autumn and winter before and after the expansion, corresponding to the three stages of seasonal variation in ET. The proportion of water bodies varies in different seasons. Before reservoir expansion (taking 2013 as an example), there was no water body inside the source area (Figure 8a to c), but after expansion (taking 2017 as an example), the proportion of water bodies in the source area was higher in spring and winter and lower in summer and autumn. The water area ratio was approximately 25.67% in the spring of 2017 (Figure 8d), so water evaporation had a higher proportion of ET. At this time, maize had not yet emerged, so the ET of the land was mainly dominated by bare soil evaporation. In summer and autumn, seasonal shrinkage of the Guanting Reservoir occurred, and the area ratio of water bodies in the LAS source area decreased to approximately 1.33% (Figure 8e), so the proportion of water body evaporation was low in the LAS source area. At this time, the maize field was in its growing season, the crop transpiration was higher than bare soil evaporation, and the ET reached its peak. In the winter of 2017, the reservoir expanded again, but the expansion was not as obvious as that in the spring, and the water area ratio in the LAS source area increased to 6.67% until November (Figure 8f). Since the

maize had been cut, the bare soil evaporation took up a higher proportion of the ET of the surrounding area. Therefore, from 2013 to 2017, the ET of the surrounding area of the Guanting Reservoir increased in spring, remained almost unchanged in summer and autumn, and increased again in winter.

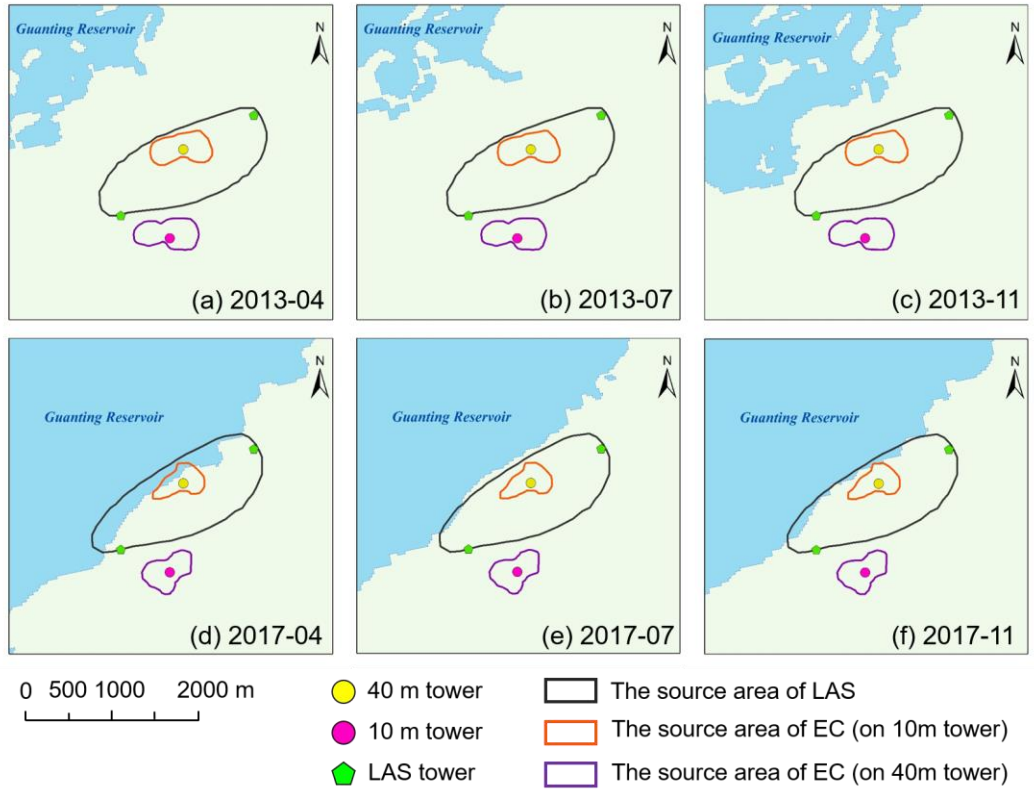

Figure 8. The 90% contribution source areas of LAS and ECs: (a, d) during spring (April), (b, e) summer (July) and (c, f) winter (November) in 2013 (before reservoir expansion) and 2017 (after expansion).

The expansion and shrinkage of the reservoir could also affect the energy and water vapor fluxes by affecting meteorological factors and underlying surface conditions in the surrounding area. In this study, net radiation (Rn) and precipitation (P) were considered to be the main meteorological factors. The underlying surface conditions include vegetation and soil factors. The average NDVI in the LAS source area was chosen to characterize vegetation growth

conditions, and surface and deep soil moisture ($Ms_{0\text{-}40\ cm}$ and $Ms_{40\text{-}160\ cm}$) represented the soil moisture conditions. The distance between the 40 m tower and reservoir (D) was also considered, which can reflect the expansion and shrinkage of the reservoir. D is the direct factor that affects ET, while meteorological and underlying surface factors are indirect factors. Since the ET in the surrounding area was dominated by crop transpiration in the growing season and by bare soil evaporation in the non-growing season, the main indirect factors affecting ET were different in those two periods. Therefore, in this study, we analyzed the correlation between the impact factors and monthly ET in both growing (May to September) and non-growing seasons (January to April, October to December). The results of the correlation analysis are displayed in Table 2 and Table 3.

Table 2 shows the results of the correlation analysis during the growing seasons. Rn had the best significant correlation with monthly ET (the Pearson correlation coefficient was 0.735), so the monthly ET was most related to the energy factors in the growing season. There was also a positive correlation between monthly ET and deep soil moisture (the correlation coefficient was 0.625), which was directly affected by the groundwater table caused by the seasonal expansion and shrinkage of the reservoir. Deep soil moisture was also related to vegetation conditions because maize could absorb deep soil moisture through its roots. Monthly ET had a positive correlation with NDVI (the correlation coefficient was 0.644). The vegetation growth condition was not only affected by agricultural activities but also controlled by net radiation and soil moisture. Therefore, during the growing season, the expansion and shrinkage of the reservoir has an indirect effect on ET by changing the net radiation, deep soil moisture and vegetation growth conditions.

Table 2. The correlation between impact factors and monthly ET during the growing season in 2013-2017

Monthly ET	D	Rn	P	NDVI	$Ms_{0\text{-}40\ cm}$	$Ms_{40\text{-}160\ cm}$
Pearson orrelation	-0.319	.735**	.487*	.644**	0.258	.625**
Significance	0.12	0.000	0.014	0.001	0.213	0.001
N cases	25	23	25	25	25	25

Note. * The correlation was significant at 0.05 level. ** The correlation was significant at 0.01 level.

In the non-growing season, the land had almost no vegetation, and the ET was mainly dominated by bare soil evaporation, so the influence of the NDVI factor was excluded from the correlation analysis. Table 3 shows the results of the correlation analysis during the non-growing season in 2013-2017. First, the monthly ET was significantly negatively correlated with the distance between the study area and reservoir, with a correlation coefficient of -0.693. This result means that during the non-growing season, reservoir expansion directly changed the proportion of water bodies in the LAS source area and became the main factor affecting ET in the surrounding area of the Guanting Reservoir. Second, the monthly ET was related to net radiation, which means that the monthly ET was also controlled by the available energy factor. In addition, ET also has a good correlation with surface soil moisture. In the non-growing season, the precipitation was low, and surface soil moisture became the major water source for bare soil evaporation. The surface soil moisture could directly affect bare soil evaporation, thus affecting ET in the non-growing season.

Table 3. The correlation between impact factors and monthly ET during the non-growing season in 2013-2017

Monthly ET	D	Rn	P	$Ms_{0\text{-}40cm}$	$Ms_{40\text{-}160cm}$
Pearson correlation	-.693*	.641**	0.156	.530**	.424*

Significance	0.012	0.000	0.372	0.001	0.012
N cases	12	33	35	35	34

Note. * The correlation was significant at 0.05 level. ** The correlation was significant at 0.01 level.

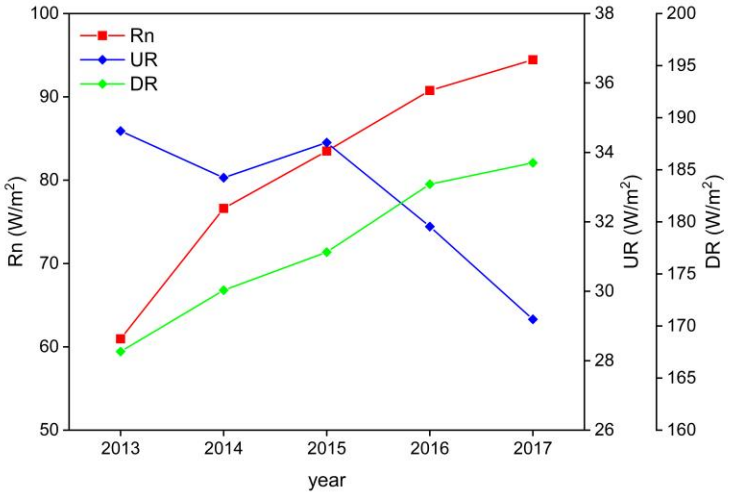

372

373 Figure 9. The variation in the net radiation (Rn) and upward shortwave radiation (UR) and downward
374 shortwave radiation (DR) at the 40 m tower from 2013 to 2017.

375 In both the growing and non-growing seasons, the monthly ET in the area surrounding the
376 Guanting Reservoir had a significant correlation with net radiation, soil moisture, and vegetation
377 conditions. On the one hand, the expansion of the reservoir increased the groundwater table and
378 then increased both surface and deep soil moisture. On the other hand, the increase in soil
379 moisture led to a decrease in albedo in the surrounding area, which decreased upward shortwave
380 radiation (UR). Meanwhile, the expansion of the reservoir also decreased the aerosols, which
381 increased the downward shortwave radiation (DR) (Figure 9). The decrease in upward radiation

and the increase in downward radiation led to an increase in the net radiation (Rn) in the surrounding area.

3.2.2 The Variation in Bowen Ratio

The Bowen ratio is the ratio of the sensible heat flux (H) to the latent heat flux (LE), which can reflect the partition of surface available energy. This ratio is also affected by environmental factors, including meteorological factors and the underlying surface conditions (such as vegetation growth conditions and soil moisture). Therefore, the Bowen ratio will also change with the interannual and seasonal expansion and shrinkage of lakes/reservoirs.

Using the H and LE data obtained by LAS, we calculated the Bowen ratio of the surrounding area of the Guanting Reservoir and then analyzed the characteristics of its interannual and seasonal variations. Figure 10 shows the variation in the Bowen ratio in the surrounding area from 2013 to 2017. In 2013 (before the expansion of the reservoir), the average Bowen ratio was approximately 2.7. Since 2014, with the expansion of the reservoir, the annual Bowen ratio has decreased year by year. Until 2016 and 2017, the Bowen ratio was almost less than 1 for the whole year and tended to be stable, and the average Bowen ratio was only approximately 0.75. In addition, in the non-growing season, the Bowen ratio was greater than 1, which means that H was larger than LE. During this period, the available surface energy was mainly consumed by turbulent heat exchange. In the growing season, the Bowen ratio was less than 1. Maize in the surrounding area of the Guanting Reservoir grew vigorously at this time, and the soil moisture and air temperature were high, so the incoming available surface energy was mainly consumed by evapotranspiration. In the growing season, the Bowen ratio did not obviously decrease from 2013 to 2017, but in the non-growing season, the Bowen ratio significantly decreased. This phenomenon was also related to the seasonal variation in the

reservoir. In the non-growing season, the proportion of water bodies in the LAS source area increased significantly (Figure 8), resulting in an increase in the LE from 2013 to 2017, as well as a decrease in the Bowen ratio. Therefore, with the expansion of the Guanting Reservoir, the partition of available energy in its surrounding area tended toward ET.

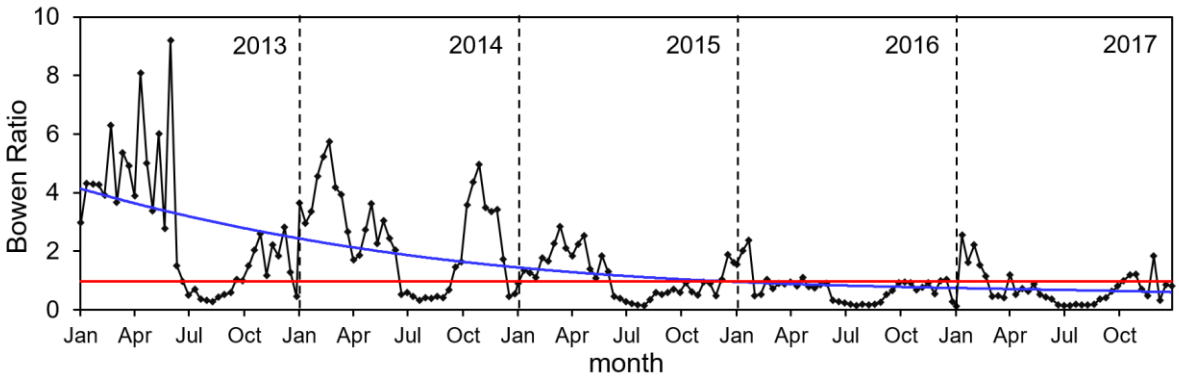

Figure 10. The variation in ten-day Bowen ratio from 2013 to 2017. The red line means the Bowen ratio is 1, and the blue line shows the variation trend of the Bowen ratio.

3.3 Variations in Energy and Water Vapor Fluxes at Different Distances from the Guanting Reservoir

In section 3.2, we analyzed the impact of the expansion and shrinkage of the Guanting Reservoir on energy and water vapor fluxes in the surrounding area. However, for the areas at different distances from the reservoir, this impact was also different. The Huailai Experiment Station has two ECs located at the 10 m and 40 m towers. The 10 m tower was further from the Guanting Reservoir, and the underlying surface in the EC source area was mainly irrigated maize field. The 40 m tower was closer to the reservoir, and its underlying surface was mainly a non-irrigated maize field. With the expansion of the reservoir, the distance between the 10 m tower and the reservoir decreased from approximately 1600 m in 2013 to approximately 930 m in

2017, and the distance between the 40 m tower and the reservoir decreased from approximately 720 m in 2013 to approximately 290 m in 2017.

Figure 11 shows the variation in the annual ET at the10 m and 40 m towers from 2013 to 2017. With the expansion of the reservoir, the ET at the 10 m tower remained almost unchanged during the five years and was stable at approximately 593 mm, while the ET at the 40 m tower continued to increase year by year. Before 2015, the 10 m and 40 m towers were both far from the Guanting Reservoir. Since the 10 m tower was in an irrigated field, the ET at the 10 m tower was larger than the ET at the 40 m tower before 2015. With reservoir expansion and the increase in ET at the 40 m tower, after 2015, the ET at the 40 m tower became larger than the ET at the 10 m tower.

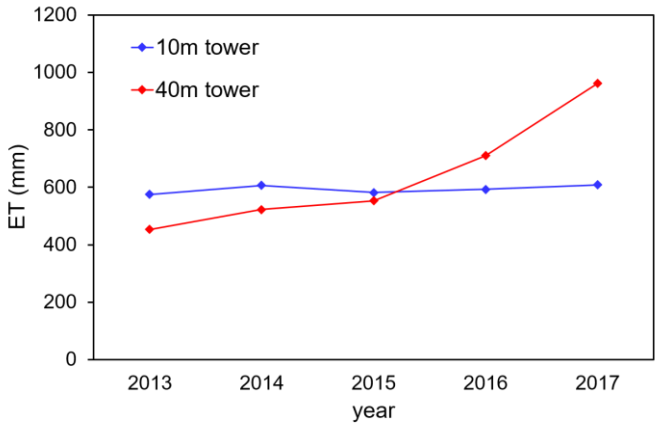

Figure 11. The variation in the annual ET at the 10 m and 40 m towers from 2013 to 2017.

The seasonal variation in ET at the 10 m and 40 m towers is shown in Figure 12. The ET at the 10 m and 40 m towers reached a peak almost at the same time in each year (in July to August), but their peak values were different. The peak value of ET at the 10 m tower in 2015-2017 was lower than that in 2013-2014, but the peak value of ET at the 40 m tower increased year by year from 2015 to 2017. Since the 10 m tower was in the irrigated field, in the growing

season (May-September) of 2013-2015, the ET at the 10 m tower was larger than that of the 40 m tower. With the reservoir expanding year by year, the ET at the 40 m tower was more affected by the expansion and led to the increase in the peak value of ET at the 40 m tower.

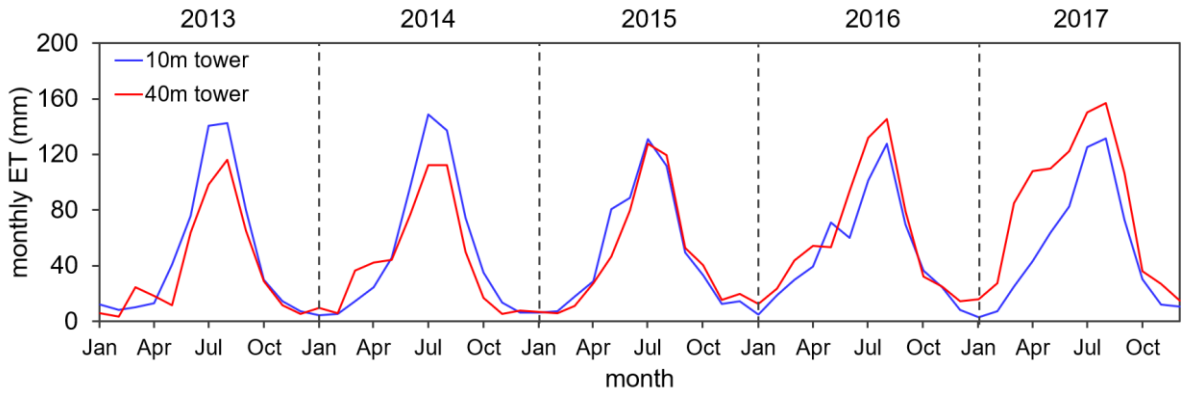

Figure 12. The seasonal variation in ET at the 10 m and 40 m towers from 2013 to 2017.

During the growing season, the reservoir has seasonal shrinkage, and there were no water bodies in the EC source areas of both the 10 m and 40 m towers (Figure 8b, e), so the ET at the 40 m tower was not significantly different from that at the 10 m tower in 2013-2017. During the non-growing season (January-April, October-December), the reservoir experiences seasonal expansion, and the ET values at the 10 m and 40 m towers were similar to each other in 2013 and 2014, but since 2015, the difference between the ET values at the two sites increased. This difference was more obvious in spring because the seasonal expansion in spring was more obvious than that in winter. On the one hand, the proportion of water bodies in the EC source area at the 40 m tower increased rapidly after reservoir expansion (for example, the water area ratio was approximately 20.42% in spring 2017, Figure 8d, f), which directly led to the increase in ET at the 40 m tower site. However, there was no water body in the EC source area at the 10 m tower in 2013-2017. On the other hand, because of reservoir expansion, the surface soil moisture at the 40 m tower site had a larger growth rate than that of the 10 m tower site, which is

shown in Figure 13a. Figure 13b indicates that the increase in net radiation was obvious at the 40 m tower, while the net radiation at the 10 m tower did not increase. Since bare soil evaporation was the major component of ET during the non-growing season, the increase in surface soil moisture was another factor affecting the increase in ET at the 40 m tower, and the increasing net radiation provided more available energy to increase ET.

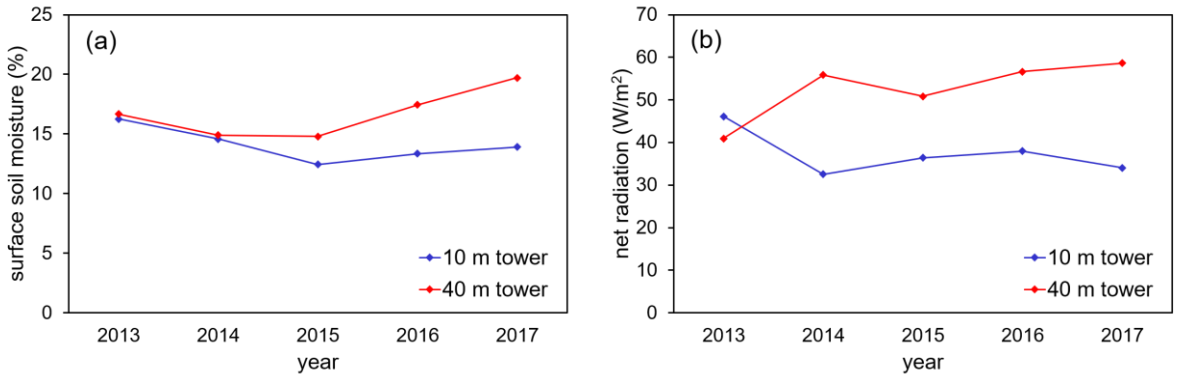

Figure 13. The seasonal variation in ET at the 10 m and 40 m towers from 2013 to 2017.

4. Conclusions

In this study, remote sensing data were used to analyze the expansion and shrinkage of the Guanting Reservoir, and LAS, EC and AWS data from the Huailai Experiment Station were used to study the variation characteristics of energy and water vapor fluxes in the surrounding area, as well as their relationships with the expansion and shrinkage of the reservoir. The main findings of this study are as follows: [1] The area of the Guanting Reservoir increased year by year from 2013-2017, and the distance between the study area and the reservoir gradually decreased year by year. The seasonal variation in the Guanting Reservoir was characterized by expansion in spring, shrinkage in summer and autumn, and expansion again in winter within one year. [2] In the surrounding area of the reservoir, the ET increased year by year with the expansion of the Guanting Reservoir and had a seasonal variation that was affected by the seasonal expansion and

shrinkage of the reservoir by changing the proportion of water bodies in the source area, net radiation and soil moisture. In the growing season, the seasonal shrinkage of the reservoir has an indirect effect on ET by changing the net radiation, deep soil moisture and vegetation growth conditions, while in the non-growing season, the seasonal expansion of the reservoir increased the proportion of the water body in the LAS source area, which was the direct factor affecting monthly ET, and the increase in Rn and soil moisture was also an important factor that affected ET. The partition of available energy in the reservoir's surrounding area tended toward ET with reservoir expansion. [3] In the surrounding area with different distances from the reservoir, the difference in ET between at the closer site and further site from the reservoir increased obviously, especially in the non-growing season. The expansion and shrinkage of the reservoir had a greater impact on the surrounding areas closer to the reservoir.

In this study, part of the remote sensing data acquired has problems such as being covered by clouds, which are more common in summer (growing season), and therefore, only the images with the most appropriate times and high quality could be selected in the study, which brings great uncertainty to the analysis.

Acknowledgments

This work was supported by the National Key Research & Development Program of China (2016YFC0500101) and the National Natural Science Foundation of China (41771364). The ground-measured turbulent heat fluxes and meteorological variables were obtained from National Tibetan Plateau Data Center (http://data.tpdc.ac.cn). Landsat OLI (Operational Land Imager) data were downloaded from the United States Geological Survey (USGS) website (https://earthexplorer.usgs.gov/).

References

Ao, Y. H., Lv, S. H., Han, B., & Li, Z. G. (2013). Analysis on micrometeorology characteristics in surface layer over Badan Jaran Desert in summer. *Plateau Meteorology*, *32*(6), 1682-1691. (in Chinese, abstract in English)

Bates, G. T., Giorgi, F., & Hostetler, S. W. (1993). Toward the simulation of the effects of the Great Lakes on regional climate. *Monthly Weather Review*, *121*, 1373-1387. https://doi.org/10.1175/1520-0493(1993)121<1373:TTSOTE>2.0.CO;2

Biermann, T., Babel, W., Ma, W. Q., Chen, X. L., Thiem, E., Ma, Y. M., & Folken, T. (2014). Turbulent flux observations and modelling over a shallow lake and a wet grassland in the Nam Co basin, Tibetan Plateau. *THEORETICAL AND APPLIED CLIMATOLOGY*, *116*(1-2), 301-316. https://doi.org/10.1007/s00704-013-0953-6

Chen, Y. P. (2007). Present situation analysis of water resources in Guanting Reservoir. *Beijing Water*, *6*, 7-11. (in Chinese, abstract in English)

Downing, J., Prairie, Y., Cole, J., Duarte, C., Tranvik, L., Striegl, R., et al. (2006). The Global Abundance and Size Distribution of Lakes, Ponds, and Impoundments. *Limnology and Oceanography*, *51*(5), 2388-2397. https://doi.org/10.4319/lo.2006.51.5.2388

Guo, H., Hu, Q., & Jiang, T. (2008). Annual and seasonal streamflow responses to climate and land-cover changes in the Poyang Lake basin, China. *Journal of Hydrology*, *355*(1-4), 106-122. https://doi.org/10.1016/j.jhydrol.2008.03.020

Guo, H., Hu, Q., Zhang, Q., & Feng, S. (2012). Effects of the Three Gorges Dam on Yangtze River flow and river interaction with Poyang Lake, China: 2003-2008. *Journal of Hydrology*, *416-417*, 19-27. https://doi.org/10.1016/j.jhydrol.2011.11.027

Haddeland, I., Heinke, J., Biemans, H., Eisner, S., Flörke, M., Hanasaki, N., et al. (2014). Global water resources affected by human interventions and climate change. *Proceedings of the National Academy of Sciences*, *111*(9), 3251-3256. https://doi.org/10.1073/pnas.1222475110

He, H. W., Zhu, Y. J., and He, C. C. (2013). Hebei Friendship Reservoir transfers water to Beijing Guanting Reservoir, plans to release water for 12 days, Accessed 9 October 2013, http://report.hebei.com.cn/system/2013/10/09/013010597.shtml. (in Chinese)

Jia, Z. Z., Liu, S. M., Xu, Z. W., Chen, Y. J., & Zhu, M. J. (2012). Validation of remotely sensed evapotranspiration over the Hai River Basin, China. *Journal of Geophysical Research: Atmospheres*, *117*, 13113. https://doi.org/10.1029/2011JD017037

Kodama, Y., Eaton, F., & Wendler, G. (1983). The Influence of Lake Minchumina, Interior Alaska, on Its Surroundings. *Archives for Meteorology, Geophysics, and Bioclimatology Series B*, *33*, 199-218. https://doi.org/10.1007/BF02275094

Kormann, R., & Meixner, F. X. (2001). An analytic footprint model for neutral stratification. *Boundary-Layer Meteorology*, *99*(2), 207-224. https://doi.org/10.1023/A:1018991015119

Lee, X. H., Liu, S. D., Xiao, W., Wang, W., Gao, Z. Q., Cao, C., et al. (2014). The Taihu Eddy Flux Network: An Observational Program on Energy, Water, and Greenhouse Gas Fluxes of a Large Freshwater Lake. *Bulletin of the American Meteorological Society*, *95*(10), 1583-1594. https://doi.org/10.1175/BAMS-D-13-00136.1

Li, X. Y., Ma, Y. J., Huang, Y., Hu, X., Wu, X. C., Wang, P., et al. (2016), Evaporation and surface energy budget over the largest high-altitude saline lake on the Qinghai-Tibet Plateau. *Journal of Geophysical Research: Atmospheres*, *121*, 10470-10485. https://doi.org/10.1002/2016JD025027

Li, X., Liu, S., Li, H., Ma, Y., Wang, J., Zhang, Y., et al. (2018). Intercomparison of six upscaling evapotranspiration methods: From site to the satellite pixel. *Journal of Geophysical Research: Atmospheres*, *123*, 6777-6803. https://doi.org/10.1029/2018JD028422

Liebethal, C., Huwe, B., & Foken, T. (2005). Sensitivity analysis for two ground heat flux calculation approaches. *Agricultural and Forest Meteorology*, *132*(3-4), 253-262. https://doi.org/10.1016/j.agrformet.2005.08.001

Liu, H. P., Zhang, Q. Y., & Dowler, G. (2012). Environmental Controls on the Surface Energy Budget over a Large Southern Inland Water in the United States: An Analysis of One-Year Eddy Covariance Flux Data. *Journal of Hydrometeorology*, *13*(6), 1893-1910. https://doi.org/10.1175/JHM-D-12-020.1

Liu, S. M., Xu, Z. W., Wang, W. Z., Jia, Z. Z., Zhu, M. J., Bai, J., & Wang, J. M. (2011). A comparison of eddy-covariance and large aperture scintillometer measurements with respect to the energy balance closure problem. *Hydrology and Earth System Sciences*, *15*, 1291-1306. https://doi.org/10.5194/hess-15-1291-2011

Liu, S. M., Xu, Z. W., Zhu, Z. L., Jia, Z. Z., & Zhu, M. J. (2013). Measurements of evapotranspiration from eddy-covariance systems and large aperture scintillometers in the Hai River Basin, China. *Journal of Hydrology*, *487*, 24-38. https://doi.org/10.1016/j.jhydrol.2013.02.025

Liu, S. M., Xu, Z. W., Song, L. S., Zhao, Q. Y., Ge, Y., Xu, T. R., et al. (2016). Upscaling evapotranspiration measurements from multi-site to the satellite pixel scale over heterogeneous land surfaces. *Agricultural and Forest Meteorology*, *230-231*, 97-113. https://doi.org/10.1016/j.agrformet.2016.04.008

Liu, X. M., Hu, F., Jiang, J. H., & Zhen, C. M. (2008). Energy budget over the water-land heterogeneous surface in Baiyangdian Region. *Chinese Journal of Atmospheric Sciences*, *32*(6), 1411-1418. (in Chinese, abstract in English)

Ma, D., Lv, S. H., Ao, Y. H., and Lin, Z. (2012), Analyses on radiation balance and surface energy budget in the Badain Jaran Desert in summer. *Plateau Meteorology*, *31*, 615-621. (in Chinese, abstract in English)

Ma, Z. G., Li, L. L., & Zhang, L. Y. (2014). Analysis of water area changes of Guanting reservoir and related factors from 1978 to 2013. *Journal of Tianjin Normal University (Natural Science Edition)*, *34*(2), 56-60. (in Chinese, abstract in English)

Min, Q. (1995). On the regulrities of water level fluctuations in Poyang Lake, *Journal of Lake Sciences*, *7*(3), 281-288. (in Chinese, abstract in English)

Nordbo, A., Launiainen, S., Mammarella, I., Leppäranta, M., Huotari, J., Ojala, A., & Vesala, T. (2011). Long-term energy flux measurements and energy balance over a small boreal lake using eddy covariance technique. *Journal of Geophysical Research: Atmospheres*, *116*, D02119. https://doi.org/10.1029/2010JD014542

Rouse, W. R., Oswald, C. J., Binyamin, J., Spence, C., Schertzer, W. M., Blanken, P. D., Bussières, N., & Duguay, C. R. (2005). The role of northern lakes in a regional energy balance, *Journal of Hydrometeorology*, *6*, 291-305. https://doi.org/10.1175/JHM421.1

Ruan, R. Z., Xia, S., Chen, Y., She, Y. J., & Yan, M. C. (2012). Change of lake nearby Linhuai Town in west bank of Hongze Lake during 1979-2006. *Wetland Sciences*, *10*(3), 344-349. (in Chinese, abstract in English)

Shadkam, S., Ludwig, F., van Vliet, M. T. H., Pastor, A., & Kabat, P. (2016). Preserving the world second largest hypersaline lake under future irrigation and climate change. *Science of The Total Environment*, *559*, 317-325. https://doi.org/10.1016/j.scitotenv.2016.03.190

Shi, X., Xiao, W. H., Wang, Y., & Wang, X. (2012). Characteristics and factors of water level variations in the Dongting Lake during the recent 50 year. *South-to-North Water Diversion and Water Science & Technology*, *5*, 18-22. (in Chinese, abstract in English)

Venäläinen, A., Heikinheimo, M., & Tourula, T. (1998). Latent heat flux from small sheltered lakes, *Boundary-Layer Meteorology*, *86*, 355-377. https://doi.org/10.1023/A:1000664615657

Vesala, T., Huotari, J., Rannik, Ü., Suni, T., Smolander, S., Sogachey, A., et al. (2006). Eddy covariance measurements of carbon exchange and latent and sensible heat fluxes over a boreal lake for a full open-water period. *Journal of Geophysical Research*, *111*, D11101. https://doi.org/10.1029/2005JD006365

Wang, T., Ochs, G. R., & Clifford, S. F. (1978). Saturation-resistant optical scintillometer to measure Cn^2. *Journal of the Optical Society of America*, *68*(3), 334–338. https://doi.org/10.1364/JOSA.68.000334

Wang, W., Shen, S. H., Liu, S. D., Zhang, M., Xiao, W., Wang, Y. W., & Lee, X. H. (2017). Mechanistic analysis of the observed energy imbalance of Lake Taihu. *Acta Ecologica Sinica*, *37*(18), 5935-5950. (in Chinese, abstract in English)

Williamson, C. E., Saros, J. E., & Schindler, D. W. (2009). Sentinels of change. *Science*, *323*(5916), 887-888. https://doi.org/10.1126/science.1169443

Xiao, K., Griffis, T., Baker, J., Bolstad, P., Erickson, M., Lee, X. H., et al. (2018). Evaporation from a temperate closed-basin lake and its impact on present, past, and future water level. *Journal of Hydrology*, *561*, 59-75. https://doi.org/10.1016/j.jhydrol.2018.03.059

Xie, C., Huang, X., Mu, H. Q., & Yin, W. (2017). Impacts of Land-Use Changes on the Lakes across the Yangtze Floodplain in China. *Environmental Science & Technology*, *51*, 3669−3677. https://doi.org/10.1021/acs.est.6b04260

Xu, Z. W., Liu, S. M., Li, X., Shi, S. J., Wang, J. M., Zhu, Z. L., et al. (2013). Intercomparison of surface energy flux measurement systems used during the HiWATER-MUSOEXE. *Journal of Geophysical Research: Atmospheres*, *118*(23), 13140-13157. https://doi.org/10.1002/2013JD020260

Yang, J. M., & Zhang, Y. W. (2016). Thoughts on water source protection of Guanting Reservoir under the coordinated development of Beijing, Tianjin and Hebei. *Beijing Water*, *1*, 48-50. (in Chinese)

Yang, Z., Cheng, C., Tan, X., Cheng, R., & Ma, Z. (2015). Analysis of water environmental capacity of Guanting Reservoir and its upstream basin. *Journal of Arid Land Resources and Environment*, *29*(1), 163-168. (in Chinese, abstract in English)

Zhang, K, C., Ao, Y. H., Qu, J. J., An, Z. S., Zu, R. P., & Han, Q. J. (2014). Influences of lake-sand dune landscape on local microclimate in Badain Jaran Desert. *Bulletin of Soil and Water Conservation*, *34*(5), 104-108. (in Chinese, abstract in English)